Structure and phase behaviour of a lyotropic mesophase system: cellulose tricarbanilate–methyl acetoacetate*

P. Haurand and P. Zugenmaier†
Institut für Physikalische Chemie der TU Clausthal, Arnold-Sommerfeld-Str. 4, D-3392 Clausthal-Zellerfeld, Germany
(Received 22 March 1990; revised 16 November 1990; accepted 16 November 1990)

Solutions of cellulose tricarbanilate (CTC) in methyl acetoacetate (MAA) have been investigated and cholesteric mesophases found above a certain concentration. Structural features as well as the phase behaviour of this lyotropic liquid crystalline system were studied. The pitch of the helicoidal cholesteric structure P decreases with higher concentration c as $P \propto c^{-m}$ with $m = 2.3$. The exponent can be correlated with the chain stiffness of the cellulosic molecule. The temperature behaviour of the pitch is in agreement with the theoretical considerations of others, if a left-handed helix conformation of a single cellulosic molecule is assumed. It can also be concluded that both steric and polar effects cause the formation of the mesophase. The thermally induced cholesteric isotropic phase transition is a first-order transition. A two-phase region separates the anisotropic and isotropic phase ranges. The beginning of the transition as well as the clearing point are shifted to higher temperatures with increasing concentration. The resulting phase diagram is qualitatively best described by the lattice theory of Flory and Warner. The higher thermotropic effect as compared to the theory is correlated to a decrease in the Kuhn segment length. The enthalpy of the phase transition rises with increasing CTC concentration and can be explained by the disappearance of polymer–polymer interactions in favour of polymer–polymer contacts.

(Keywords: cellulose tricarbanilate; methyl acetoacetate; liquid crystalline solution; helicoidal structure; optical rotatory dispersion; phase behaviour; polarization microscopy; refractometry; differential scanning calorimetry)

INTRODUCTION

Cellulose and its derivatives form thermotropic[1–5] and/or lyotropic[6–9] liquid crystalline phases with suitable solvents. Two approaches may be used in the experimental evaluation of a theory of polymeric lyotropic mesophases: (1) the substituents on the cellulosic backbone are varied and the derivatives investigated in one solvent; (2) different solvents or solvent systems are used which show good solvent characteristics for a single cellulose derivative.

In this manner, the influence of substituents or solvents on the formation, structure and properties of mesophases may be systematically studied. A clarification of these correlations is also of great interest for the application of the products.

As shown elsewhere, cellulose tricarbanilate (CTC) forms lyotropic liquid crystals in highly concentrated solutions of ketones[10] and ethylene glycols and derivatives thereof[11–13]. A new class of solvents for this cellulose derivative is presented by the acetoacetic acid esters. In methyl-acetoacetate (MAA) as well as in ethyl esters (EAA) of this series of solvents, cholesteric liquid crystalline phases are observed above a critical concentration and reflect light in the visible range.

In this paper CTC–MAA will be characterized with regard to its structure and phase behaviour. The pitch of the helicoidal supermolecular structure correlates with the reflection wavelength, determined from optical rotatory dispersion (ORD) and ultraviolet (u.v.)-visible (vis.) spectra, and is tested against the reflection colours of planar structures using a polarization microscope. Temperature-dependent refractometric measurements on surface oriented samples allow the determination of the order parameter and give information on phase behaviour. The anisotropic-isotropic phase transition is studied with additional differential scanning calorimetry (d.s.c.) and thermomicroscopic investigations and the different methods used are compared. The influence of the molar mass distribution of the polymeric material on the thermal behaviour of the sample is discussed.

EXPERIMENTAL

The CTC was synthesized by a reaction of cellulose (Avicel) with phenyl isocyanate in pyridine. The degree of polymerization (DP) was measured by gel permeation chromatography (g.p.c.) as $DP = 175$ with a polydispersity of molar mass distribution $M_w/M_n = 6$. A CTC fraction with $DP = 155$ and $M_w/M_n = 1.4$ was available and introduced for comparison. The solvent was purchased from Fluka and used without further purification.

The liquid crystalline solutions were prepared by weighing the required amount of CTC ($DP = 175$) in an Eppendorf vessel, adding the solvent and stirring the mixture at room temperature. The samples were stored for 6 h to obtain good homogeneity and stirred again. A series of 21 different concentrations were used, ranging from 0.4 to 1.4 g dry CTC/1 ml MAA in increments of 0.05 g ml^{-1}.

* Dedicated to Professor Dr W. Burchard on the occasion of his 60th birthday
† To whom correspondence should be addressed

0032-3861/91/163026-12

Spectroscopic measurements

The u.v.-vis.-near infra-red (n.i.r.) transmission curves were obtained using a spectrometer (Bruins Instruments). The reflection wavelengths of the cholesteric structures were determined as a function of concentration and temperature. Optical rotatory dispersion spectra provided, besides the reflection wavelength, the handedness of the helicoidal cholesteric structure. The measurements were carried out in a Perkin-Elmer polarimeter MC 241 in the wavelength range from 300 to 700 nm. A simple relation between reflection wavelength, λ_0, and the pitch of the structure, P, exists when a homeotropic orientation of the molecules (planar structure) is provided and the light beam directed parallel to the optical axis:

$$\lambda_0 = \bar{n}P \quad (1)$$

where $\bar{n}$ is the mean refractive index of a nematic layer of the cholesteric structure.

The homeotropic orientation was obtained by preparing the liquid crystalline solutions between two quartz plates which had been rubbed in one direction with a cotton cloth. The thickness of the samples can be easily varied with the use of spacer foils. Optimal planar structures of the CTC–MAA system were observed with 10 μm foils.

Refractometry

The ordinary and extraordinary refractive indices of the anisotropic solutions were determined by an Abbé refractometer (589 nm). Homeotropic planar structures are essential and produced by rubbing the surfaces of the prisms with a cotton cloth in the longitudinal direction. The samples were coated as a thin layer using a spatula. The temperature was controlled to within ± 0.1°C using a thermostat connected to the prisms.

Polarization microscopy

The planar structures were studied using a polarization microscope (Olympus BH-2) equipped with a Mettler hot stage FP 5 as a function of temperature, and the anisotropic–isotropic phase transition was easily observed. Heating steps of 5°C were applied in the anisotropic phase, and the reflection colour was recorded with an Olympus OM-2 camera after the equilibrium structure, normally after 5–15 min, was obtained. Smaller temperature steps (<0.5°C) were used in the vicinity of the phase transition to ensure a good detection of the phase separation. The formation of the isotropic phase was easier to observe if the analyser was turned 20° from the crossed position. The temperature was only increased when the structure or the size of the coexisting phases showed no further change to reduce kinetic hindrance as much as possible.

Differential scanning calorimetry

A Perkin-Elmer DSC-7, equipped with a liquid nitrogen based cooling system, was used to study the phase behaviour in addition to the polarization microscopic investigations. Liquid crystalline samples from the concentration series (20 ± 0.5 mg) were placed in 50 μl aluminium pans which were closed with a welded lid. An identical aluminium pan filled with pure solvent served as a reference. Heating and cooling curves were recorded for all the liquid crystalline solutions in a temperature range of 10–110°C (283–393 K). The CTC and pure solvent show no phase transition in this temperature range. The scanning rate was varied from 9 to 49°C min^{-1}. The onset (T_{onset}) and peak (T_{peak}) temperatures as well as the enthalpy changes, ΔH, were determined from the curves and evaluated for an interpretation of phase transitions. The samples were weighed again after the d.s.c. runs to ensure that no weight loss occurred due to evaporation of MAA during the measurements.

RESULTS AND DISCUSSION

Clear isotropic solutions are observed for concentrations $c \leqslant 0.55$ g CTC ml^{-1} MAA at room temperature and at slightly higher concentrations are succeeded by phase separation, shown by a slight opaqueness of the solution. A completely anisotropic system is obtained above 0.65 g ml^{-1}. The oriented liquid crystalline samples reflect visible light in the concentration range from 0.65 to 1.2 g ml^{-1}. The reflection colour changes from red to blue with increasing concentration. Above 1.20 g ml^{-1} a reflection of visible light was no longer observed and the solution appears highly viscous.

Spectroscopy

As cholesteric phases exhibit a helicoidal structure, the optical rotatory power Θ shows a characteristic dependence on wavelength (ORD), which was theoretically predicted by de Vries[14]. The dispersion behaviour of variously concentrated CTC–MAA solutions, measured at 20°C, is represented in *Figure 1*. The crossing point of the curve with the λ axis ($\Theta = 0$) determines the reflection wavelength λ_0, which shifts to lower wavelengths with higher concentrations. A left-handed twist of the structure for the CTC MAA systems has to be assumed on the basis of negative Θ values in the range $\lambda < \lambda_0$, according to theoretical considerations.

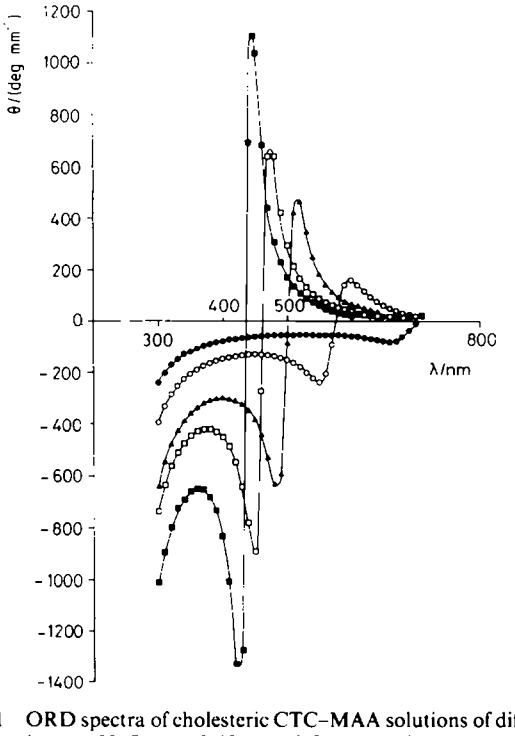

Figure 1 ORD spectra of cholesteric CTC–MAA solutions of different concentrations at 20°C: (●) 0.65; (○) 0.75; (▲) 0.85; (□) 0.95; (■) 1.05 g ml^{-1}

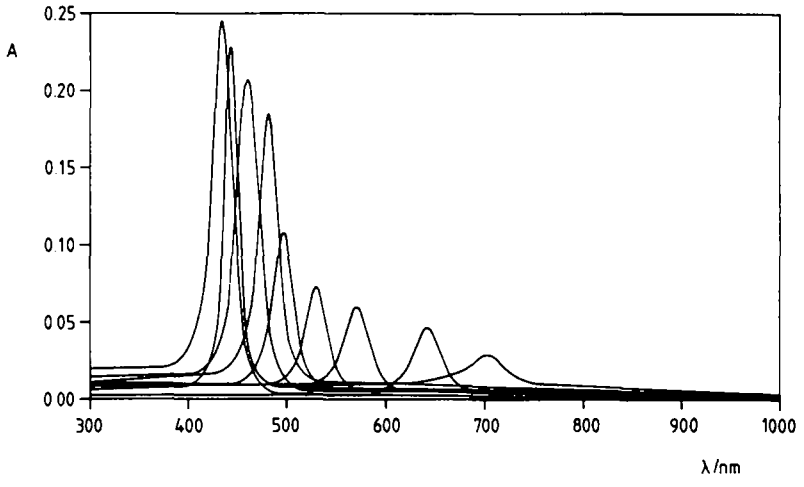

Figure 2 Absorbance spectra of cholesteric CTC–MAA solutions with different concentrations at 20°C (from right to left: 0.65, 0.7, 0.75 ... 1.05 g ml^{-1})

Table 1 Comparison of reflection wavelengths determined using different methods for various concentrations of CTC–MAA solutions

Concentration (g ml^{-1})	λ_0 (u.v.–vis.–n.i.r.) (nm)	λ_0 (ORD) (nm)	λ_0 (by λ_{max}) (nm)
0.65	704	702	750
0.70	641		
0.75	570	576	636
0.80	530		
0.85	496	501	566
0.90	482		
0.95	461	462	530
1.00	445		
1.05	435	437	509

If the ORD curves are considered as a whole, it is observed that they deviate from the theoretically calculated ones analogously to other liquid crystalline CTC solutions[13]. Especially large differences are observed in the range $\lambda \ll \lambda_0$. This leads to the conclusion that the relation between the maximum of the curve λ_{max}, ahead of the reflection wavelength λ_0, and λ_0 ($\lambda_{max} = \lambda_0/\sqrt{2}$)[15] derived from the de Vries equation does not hold for the CTC–MAA system.

The selective reflection of cholesteric phases is also available by determination of the maximum of corresponding u.v.-vis. absorption curves. Such curves are depicted for CTC–MAA solutions in the concentration range from 0.65 to 1.05 g ml^{-1} at 20°C in *Figure 2*. The samples with $c = 1.1$–1.2 g ml^{-1} still reflect visible light but their viscosity is too high for the formation of well oriented planar structures, necessary for spectroscopically meaningful evaluations. The reflection wavelength shifts to lower λ_0 values with increasing concentration in accordance with the ORD measurements. The size and sharpness of the u.v.-vis. peaks increase with higher concentration and are correlated with the stability of the liquid crystalline phase, degree of order and the number of repeat units (pitches) within the thickness of the sample layer. The distances between peak maxima increase when the isotropic phase approaches. These two observations also hold for the ORD curves. Equation (1) allows the determination of the pitch P from the reflection wavelength λ_0. The experimental values are given in *Table 1*. The error in the measurements can be estimated to be $< \pm 3$ nm due to excellent homeotropic

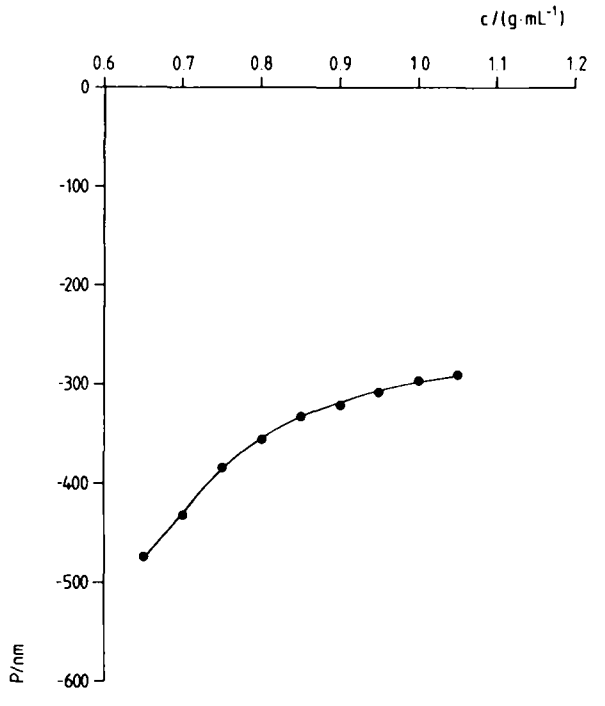

Figure 3 Dependence of pitch P on concentration c for CTC–MAA solutions at 20°C

preparation of the samples carefully checked by polarization microscopy. This small error is essential for the following evaluation of the experimental data.

The evaluation of the pitch as a function of concentration (*Figure 3*) reveals the existence of two clearly separated ranges with different gradients. Normally, the concentration dependence of the pitch is empirically described in the whole existence range of the lyotropic mesophase by:

$$P = kc^{-m} \tag{2}$$

or

$$\log P = \log k - m \log c \tag{2a}$$

where k is a constant and m is an exponent which may be determined in a double logarithmic plot (cf. equation (2a)) as the slope of a straight line.

The exponent m depends on the stiffness of the

molecules, on the kind of solvent used, the temperature and molar mass. Stiff polybenzyl γ-glutamate (PBLG) in dioxane[16] led to a value of $m=2$; for semiflexible hydroxypropyl cellulose (HPC) in water[17] $m=3$. *Figure 4* represents the dependence of pitch on concentration (c in wt%) on a double logarithmic scale at five temperatures. The corresponding m values are listed in *Table 2*. According to *Table 2*, m is independent of temperature for small concentrations (38–44 wt%) and has a value of ~2.4 which is between the values found for PBLG and HPC. The lower m values at higher concentrations (44–49.5 wt%) lead to the conclusion that a stronger twisting of the nematic sheets is hindered. The hindrance can be removed by an increase in temperature. A single concentration gradient (slope) is found with $m=2.3$ above 35°C. This limiting value is characteristic for the CTC–MAA system and may signify a higher chain stiffness of CTC as compared with HPC.

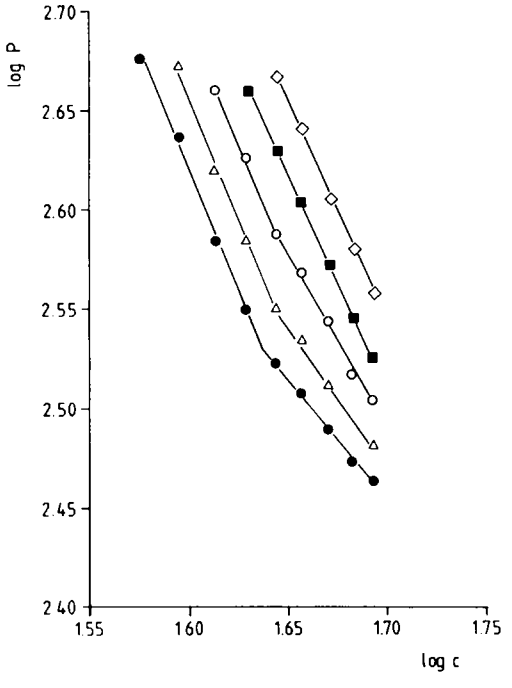

Figure 4 Plot of pitch P *versus* concentration c (wt%) on a logarithmic scale at different temperatures: (●) 20; (△) 25; (○) 30; (■) 35; (◇) 40°C

The typical temperature behaviour of the reflection wavelength of the CTC–MAA solutions for a sample with $c=1.0\ \mathrm{g\ ml^{-1}}$ is shown in *Figure 5*. The curves were recorded from 10 to 55°C in steps of 5°C in a u.v.-vis. spectrometer. The reflection wavelength λ_0, taken as the maximum of the curves, increases with temperature. The peak heights have a maximum at a characteristic temperature which is 15°C for concentrations from 38 to 43 wt% and 20°C for higher concentrations. It is noteworthy that gradient changes in temperature and concentration of the pitch lie in the same concentration range of the anisotropic solutions. An increase in reflection wavelength and consequently a negative temperature gradient of the negative pitch (*Figure 6*) at first glance contradicts the theory of Kimura *et al.*[18], which forbids $P^{-1}\,(\mathrm{d}P/\mathrm{d}T)>0$ for cholesteric phases with left-handed helicoidal twist. Kimura *et al.* reached this conclusion by an estimation of the influence of polar and steric effects on the twisting power P^{-1} using the assumption that right-handed molecular helices (conformations) are the basic units of the liquid crystalline phases. This premise is reflected in a positive sign of the parameter Q in equation (3), in which the twisting power

Table 2 Exponent m of equation (2) as a function of temperature in two concentration ranges

Concentration (wt%)	Temperature (°C)	m
38–44	20	2.4
	25	2.4
	30	2.4
	35	2.3
	40	2.3
44–49.5	20	1.1
	25	1.4
	30	1.6
	35	2.3
	40	2.3

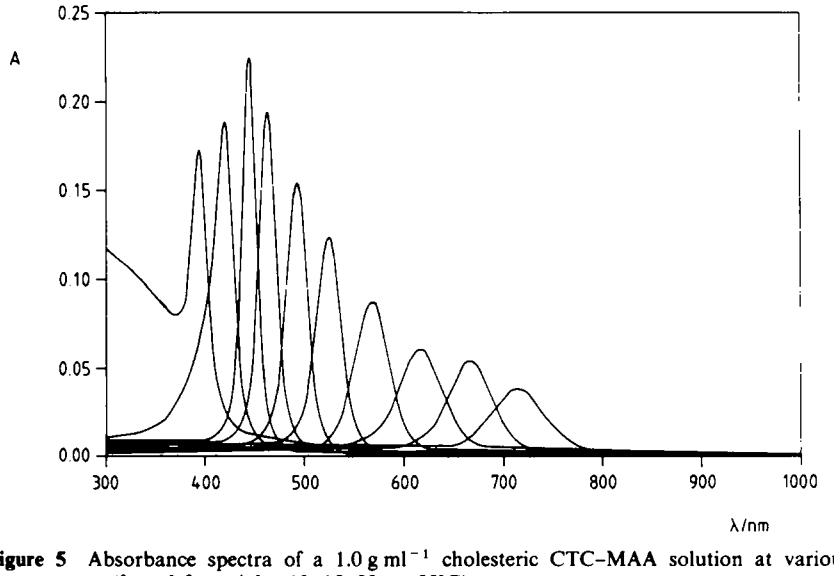

Figure 5 Absorbance spectra of a $1.0\ \mathrm{g\ ml^{-1}}$ cholesteric CTC–MAA solution at various temperatures (from left to right: 10, 15, 20 ... 55°C)

P^{-1} is related to the temperature T by[19]:

$$P^{-1} = T_n Q T^{-1} - Q = Q(T_n/T - 1) \quad (3)$$

where T_n is the inversion temperature of the supermolecular cholesteric structure, i.e. for $P^{-1} = 0$, in K.

A plot of twisting power P^{-1} against inverse temperature T^{-1} leads to a straight line with negative slope and a positive intersection on the T^{-1} axis from which $T_n = 130°C$ can be derived (*Figure 7*). Since T_n lies above the clearing temperature of the system which means $T < T_n$ in equation (3), the parameter Q must have a negative sign for a left-handed helicoidal supermolecular structure with $P < 0$. Consequently the polymeric chain has to form a left-handed helix (conformation).

A left-handed chain conformation introduced into Kimura's considerations[18] leads to an increase as well as a decrease in the pitch with temperature (*Figure 8*). A comparison of *Figure 8* with *Figure 6* leads to the conclusion that besides steric effects, polar effects play an important role in the formation of liquid crystalline phases in the CTC–MAA system.

Polarization microscopy

Polarization microscopic observations provide additional information on the spectroscopically determined

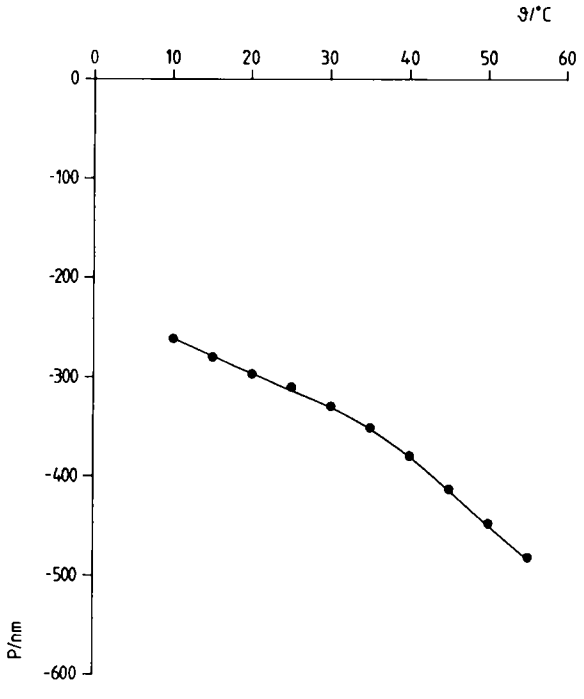

Figure 6 Dependence of pitch P on temperature of a 1.0 g ml^{-1} CTC-MAA solution

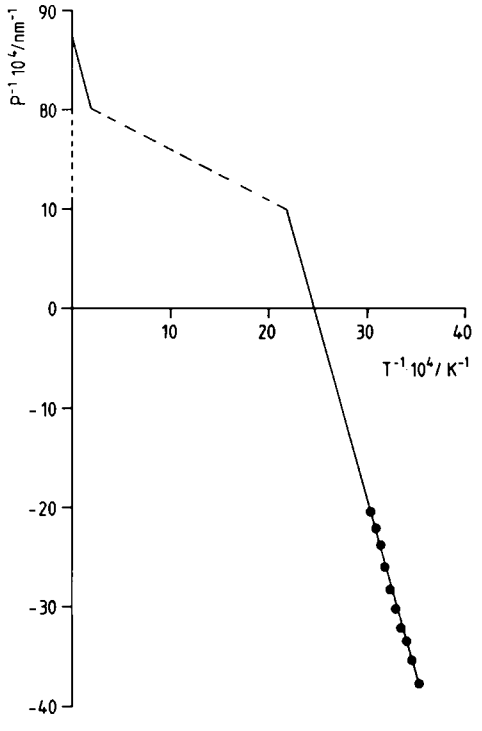

Figure 7 Twisting power P^{-1} as a function of T^{-1} of a 1.0 g ml^{-1} CTC-MAA solution

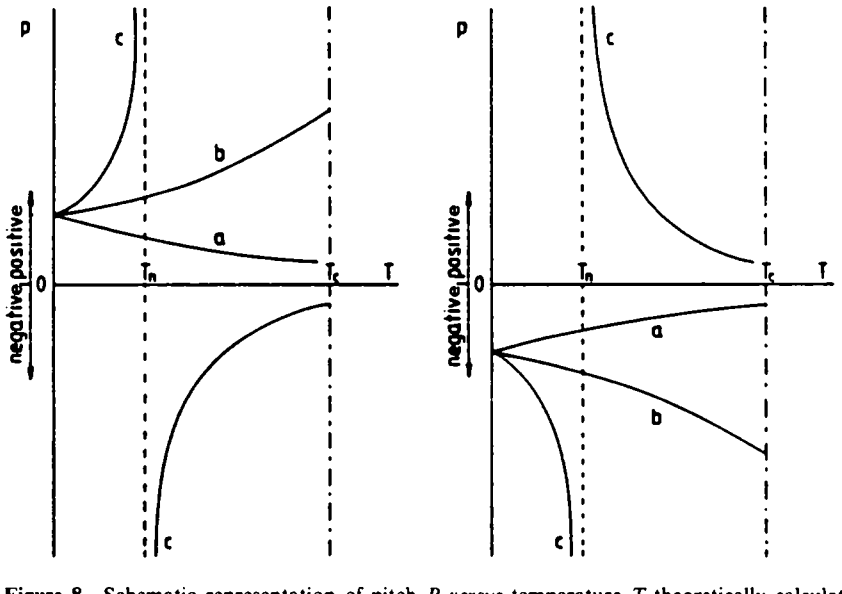

Figure 8 Schematic representation of pitch P *versus* temperature T theoretically calculated according to Kimura *et al.*[18] for $Q > 0$ (left) and $Q < 0$ (right): (a) predominant polar interactions; (b) polar and steric effects; (c) predominant steric effects

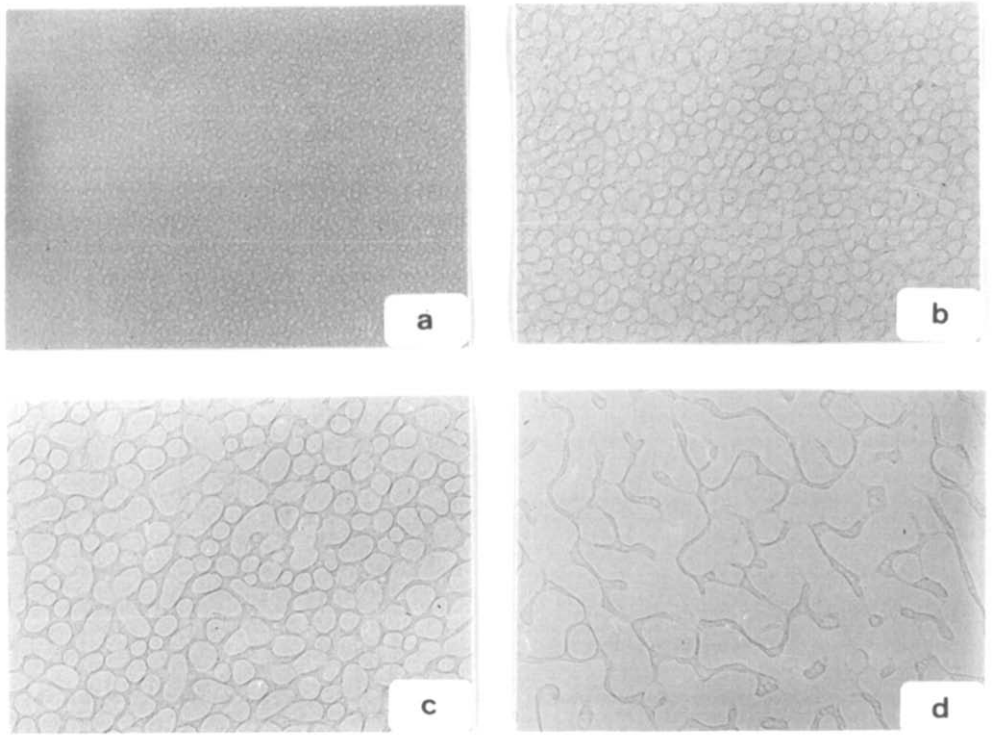

Figure 9 Polarization microscopy micrographs of the cholesteric–isotropic phase transition of a 0.7 g ml^{-1} CTC–MAA solution with the analyser 20°C out of the crossed position at different temperatures: (a) 28; (b) 34; (c) 40; (d) 46°C. Magnification ×98

reflection behaviour. The colour of the planar structures of CTC–MAA changes, when observed between crossed polars parallel to the optical axis, from blue violet to dark red with increasing temperature and spans the same colour range with decreasing concentration. The formation of small isotropic droplets in an anisotropic matrix marks the beginning of the cholesteric–isotropic phase transition on heating for each concentration occurring at a characteristic temperature. The size of the coexisting phases changes with increasing temperature in favour of the isotropic solution. The last liquid crystalline structure disappears at the clearing temperature, T_c. Micrographs from the polarization microscopy studies are shown for a 0.7 g ml^{-1} CTC–MAA system in *Figure 9*. The growth of isotropic droplets, clearly visible with increasing temperature, indicates the exclusion of an isothermal anisotropic–isotropic phase transition, since kinetic hindrances can be neglected. There exists a two-phase region between the anisotropic and isotropic solution, and its size is dependent on the composition of the sample. The resulting phase diagram for CTC–MAA is given in *Figure 10*.

A two-phase region is expected according to Gibbs' phase rule for a binary mixture at constant pressure[20]. A liquid crystalline and isotropic phase are in equilibrium at the phase transition, which is monovariant and non-isothermal. The size of the two-phase region (temperature range) decreases with concentration. The coexistence lines of the diagram in *Figure 10* can be approximated by three straight lines, with each slope becoming smaller at higher concentration. The concentration ranges between the break points correspond to those for which break points in the temperature and concentration gradients of the pitch have been observed. The experimentally determined phase behaviour of CTC–MAA has been compared with the results of

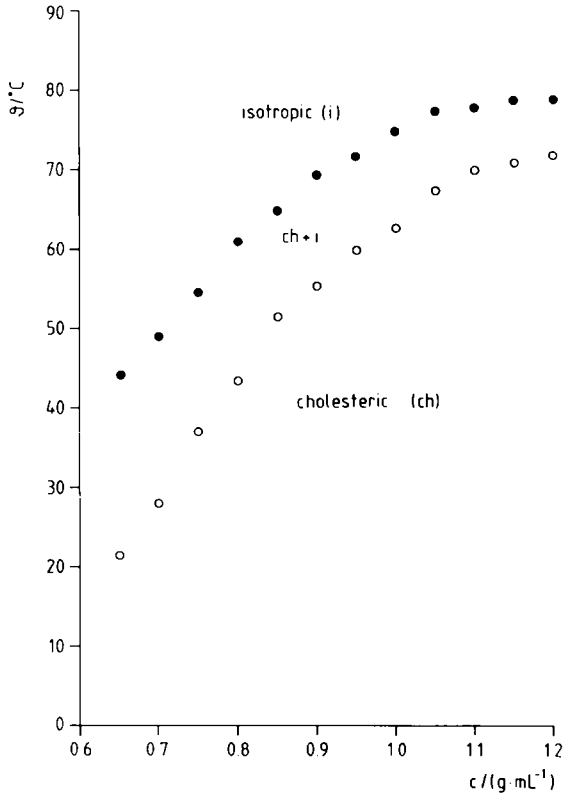

Figure 10 Phase diagram of CTC–MAA determined by polarization microscopic observations

different theoretical considerations in *Figure 11*. Theoretical models are evaluated using the following approximations: (1) the virial approximation (Onsager[21], Khokhlov and Semenov[22]); and (2) the lattice approximation (Flory and co-workers[24–28]).

Onsager considered the phase separation to be derived

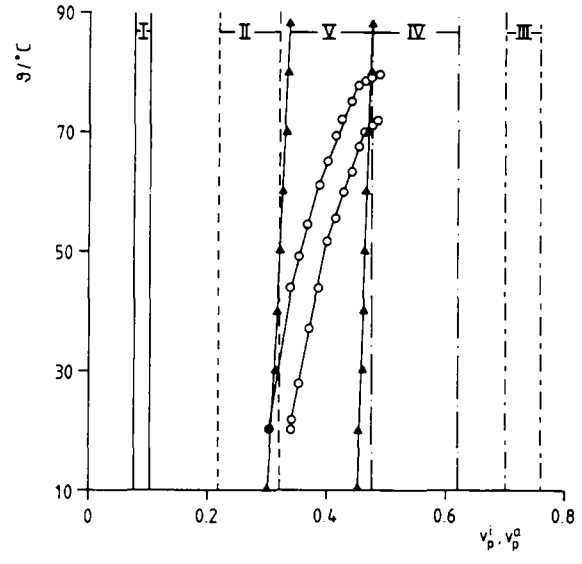

Figure 11 Experimentally (○) determined phase boundaries for the system CTC–MAA and comparison with various theoretical models: (I) theory of Onsager for stiff rods; (II) theory of Khokhlov and Semenov for freely jointed segments; (III) theory of Khokhlov and Semenov for worm-like molecules; (IV) theory of Flory, athermic and aspect ratio $x = 15$; (V) theory of Flory and Warner with anisotropic interactions and $x = 15$ (▲); ϑ temperature in °C; v_p^i, v_p^a, cf. *Table 3*

from the free energy of the total system with the second virial coefficient of the interactions between rods as the major part[21] which is exclusively of steric nature. Higher order terms are omitted for the low polymer concentrations considered. This model is often referred to as the 'second virial approximation'. Khokhlov and Semenov extended these considerations for stiff rods (region I in *Figure 11*) to semiflexible polymers[22]. The kind of flexibility present in the chains strongly influences the phase behaviour. For worm-like molecules with homogeneously distributed flexibility the merging of the chains to an anisotropic phase occurs at higher concentrations (region III) compared to a polymeric chain composed of flexibly jointed stiff segments (region II). Furthermore, the two-phase region is smaller and the degree of order essentially lower at the phase transition. The results of the three regions are summarized in *Table 3*.

A Kuhn segment length of 300 Å has been assumed for CTC with a diameter of 20 Å for the chain from a conformational study[23], leading to an aspect ratio of $x = 15$.

The phase behaviour of liquid crystals has also been considered on the basis of a lattice model with the atoms placed on a cubic lattice, and the phase separation determined by the partition function. Flory introduced[24] a model for stiff rods with an aspect ratio x in 1956 and published further details in a later paper[25]. Steric repulsion between the dissolved species is exclusively responsible for the ordering in lyotropic liquid crystalline phases (athermic case). The aspect ratio of the rods determines the phase separation. These considerations are transferred to semiflexible chains by replacing the total chain length by the Kuhn segment length in calculating the aspect ratio[26]. The total length of the molecules plays a minor role in the calculation of the critical concentration and anisotropy effects. The equilibrium concentrations, according to the lattice theory, are depicted for the athermic case in *Figure 11* (region IV). The values have been calculated with the data of Figure 4 in reference 25 for $x = 15$. The results obtained do not agree with the experimental data. Further development of the lattice theory by considerations of orientation-dependent attractive interactions has been conducted for thermotropic liquid crystals by Flory and Ronca[27] and for lyotropic systems by Warner and Flory[28]. The results of the latter theory have been tested for the CTC–MAA system. The theoretical phase diagram for $x = 15$ shows[29] that the athermal limiting value $v_p^i = 0.475$ decreases to $v_p^i = 0.31$ in agreement with the measured value at 20°C and the quantity $xT^*/T \approx 5.4$ is still within the small region of coexistence. A critical temperature of $T^* = 106$ K results for $x = 15$ and $T = 293$ K and represents a measure for the anisotropic interactions. The value for T^* seems reasonable in comparison with theory[27] and the result obtained for other cellulose derivatives[29]. With $T^* = 106$ K and the theoretical phase diagram for $x = 15$, the volume fractions of the coexisting phases have been calculated in the temperature range from 20 to 90°C (region V in *Figure 11*).

The second virial approximation does not describe the experimental results for the model of stiff rods, for freely jointed segments or for worm-like chains as clearly demonstrated in *Figure 11*. It might be that the necessary concentration for the formation of the liquid crystalline phase is too high for the CTC–MAA system in which case the omitted terms have to be considered in the virial expansion. Besides the polymer–solvent contacts polymer–polymer interactions may play an important role in the considered temperature range and since CTC possesses anisotropic polarizability, the dispersion forces depend on the relative orientation of the chain segments to one another. Energetically the parallel orientation of the molecules is favoured and with it, the formation of the liquid crystalline phase. These considerations are not included in the second virial approximation and may contribute to the poor agreement with experimental data.

The experimental results are best qualitatively described by a lattice model which considers steric repulsion and anisotropic dispersion forces. However, quantitatively there are deviations from the theory with regard to the temperature dependence of v_p^a and v_p^i (thermotropic effect) and the width of the two-phase region. The equilibrium concentrations, calculated with $T^* = 106$ K, increase by ~8% in the temperature range from 20 to 70°C, the measured values by 38%. This high thermotropic effect may be a consequence of a decrease in Kuhn segment length and with it the corresponding aspect ratio with increasing temperature[30]. The two-phase region is amazingly small, characterized by the ratio $v_p^a/v_p^i = 1.12$, in spite of the wide molar mass distribution of CTC ($M_w/M_n = 6$) used in this investigation. This ratio is well below the calculated value for

Table 3 Predicted results from the virial approximation used for *Figure 11*

	v_p^i	v_p^a	S	v_p^a/v_p^i
Region I	3.34/x	4.49/x	0.84	1.34
Region II	3.25/x	4.86/x	0.87	1.50
Region III	10.48/x	11.39/x	0.49	1.09

Abbreviations: v_p^i, v_p^a, volume fraction of the polymer in the isotropic and anisotropic phases in equilibrium, respectively; S, degree of order of the liquid crystalline structure; x, aspect ratio, length to diameter of a segment or stiff rod, respectively

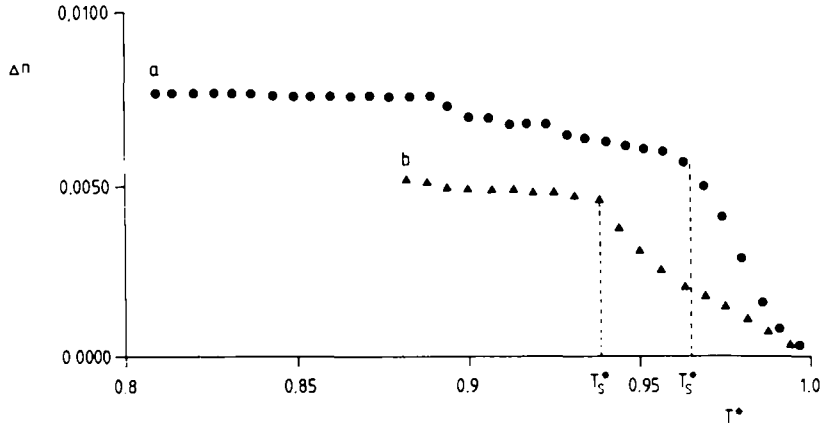

Figure 12 Birefringence Δn as a function of reduced temperature T^* ($T^* = T/T_c$) of a CTC–MAA solution with c: (a) 1.0; (b) 0.7 g ml^{-1}

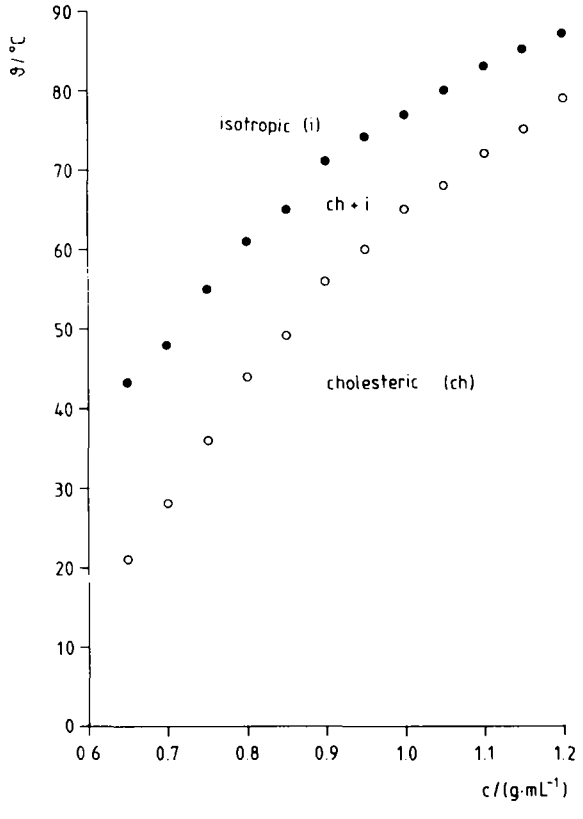

Figure 13 Phase diagram of CTC MAA determined by refractometry

monodisperse rods with $x = 15$ (region V), which leads to $v_p^a/v_p^i = 1.45$. Normally, the two-phase region is expected to be much larger for polydisperse systems, and its width varies with the molar mass distribution[31–33]. The experimental results suggest that CTC forms semiflexible chains, and the phase behaviour is solely governed by the size of a stiff segment and not by the molar mass and consequently not by the molar mass distribution. The extremely small ratio v_p^a/v_p^i in comparison with monodisperse stiff rods cannot be interpreted at present. Similar experimental results have also been observed for other cellulose derivatives[34].

Refractometric measurements

The refractive index of the extraordinary ray n_e is larger than that of the ordinary ray n_0 for all uniaxial cholesteric CTC–MAA solutions, which means they possess optically positive character. The value of the birefringence $\Delta n = n_e - n_0$ varies with concentration and temperature of the lyotropic liquid crystalline phases. The temperature dependence of Δn is represented as a function of reduced temperature T^* ($T^* = T/T_c$) for two samples with $c = 1.0$ and 0.7 g ml^{-1} in *Figure 12*. The shapes of the two curves are characteristic for the entire series of experiments. The birefringence increases with higher CTC concentration. A characteristic temperature T_s^* is found with a break in the curves. Change of temperature in the range $T^* < T_s^*$ results in small variations of the birefringence. A steep drop of birefringence occurs in the range $T_s \leqslant T^* \leqslant 1$ which represents the biphasic region. The loss in birefringence above T_s^* is caused by the disappearance of cholesteric parts of the solution in favour of the isotropic solution. The phase transition is completed at T_c ($T^* = 1$) and the solution is solely isotropic with $\Delta n = 0$. The range of coexistence between anisotropic and isotropic phases is subsequently marked by $(1 - T_s^*)$ and becomes smaller with increasing concentration of the cellulose derivative. *Figure 13* shows the corresponding phase diagram determined by refractometric measurements. The coexistence lines represent the break points T_s^* and T_c of variously concentrated CTC–MAA solutions. A comparison with the results from the polarization microscopy study (*Figure 10*) leads to good agreement. It should be noted that the change in slope is less pronounced for the samples with $c = 1.1$–1.2 g ml^{-1} which leads to higher temperature values in *Figure 13*.

Using the extrapolation method of Haller[35] the temperature dependence of the refractive indices leads to the order parameter S. *Figure 14* shows S as a function of reduced temperature T^* for solutions with $c = 0.7$ and 1.0 g ml^{-1}. The lower curve ($c = 1.0$ g ml^{-1} demonstrates the influence of a smaller molar mass distribution on the order parameter. The influence of concentration and molar mass distribution on size and temperature seems negligible within the liquid crystalline region. A value of $S = 0.5$ was found at the breakpoint T_s^* for samples in the concentration range of 0.7–1.1 g ml^{-1}. The higher concentrated solutions exhibit a smaller order parameter ($S = 0.41$) as a result of their higher viscosity. In the biphasic region, the order parameter decreases according to the decrease in the birefringence with higher temperature. The biphasic region becomes smaller not only with increasing concentration, but also at the same

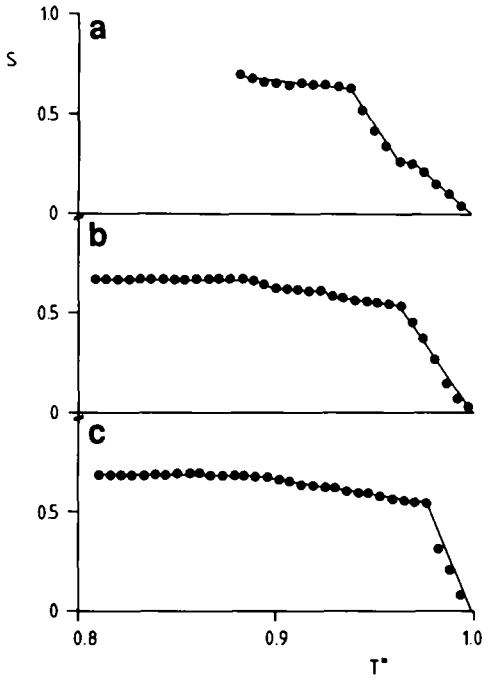

Figure 14 Degree of order S as a function of reduced temperature T^* of CTC–MAA with: (a) $c = 0.7$ g ml^{-1}, $M_w/M_n = 6$; (b) $c = 1.0$ g ml^{-1}, $M_w/M_n = 6$; (c) $c = 1.0$ g ml^{-1}, $M_w/M_n = 1.4$

concentration with decreasing molar mass distribution (cf. *Figures 14b* and *c*). The size of the molar mass distribution influences the phase behaviour for the system CTC–MAA in contrast to the theory of Flory *et al.*[25–28] for semiflexible molecules. A more precise description requires further investigation using a series of concentrations of various CTC fractions.

Differential scanning calorimetry

Important information concerning phase behaviour of the lyotropic CTC–MAA system is provided by the site, form and size of d.s.c. peaks. The d.s.c. curves on heating and cooling are represented for various concentrations of solutions for a series of experiments from 0.7 to 1.2 g ml^{-1} using a constant heating rate of 20°C min^{-1} in *Figure 15*. The exothermic peaks (*Figure 15b*) for all concentrations are considerably sharper than the corresponding endothermic peaks (*Figure 15a*) for the same concentration. This phenomenon can be related to the fact that the isotropic–anisotropic phase transition is strongly controlled by kinetics. The isotropic solution supercools to a non-equilibrium system, which turns by spontaneous orientation of the CTC molecules into the liquid crystalline state on further cooling[36]. Since equilibrium states are not passed through on cooling because of kinetic hindrance, the anisotropic–isotropic phase transition has to be considered for an evaluation

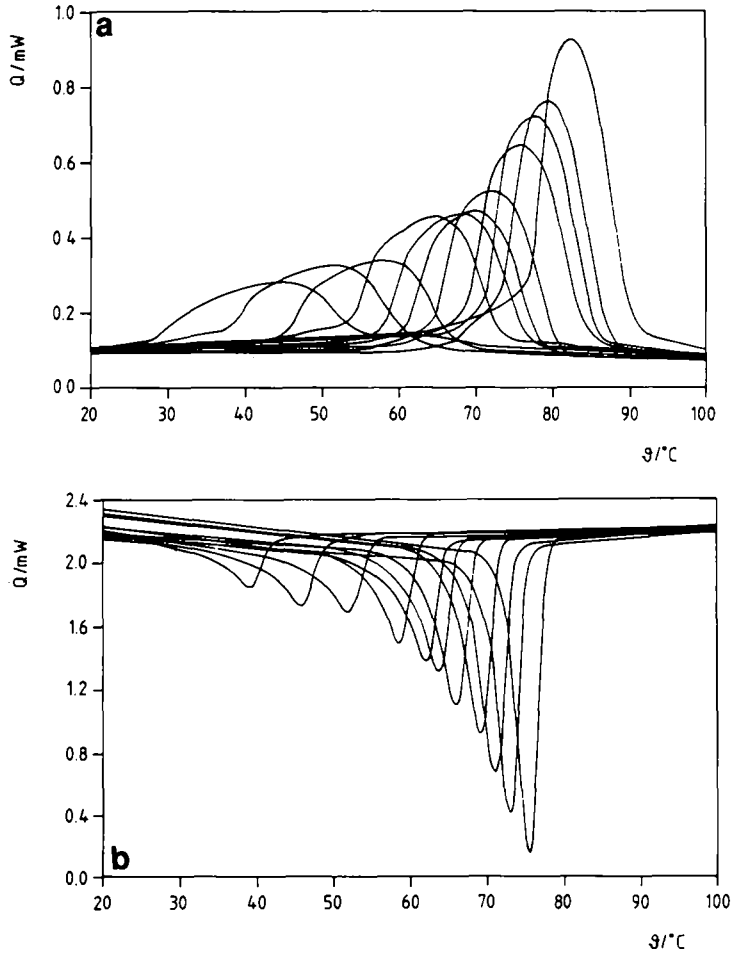

Figure 15 Differential scanning calorimetry thermograms of lyotropic liquid crystalline CTC–MAA solutions at various concentrations (from left to right: 0.7, 0.75 ... 1.2 g ml^{-1}): (a) on heating (rate 20°C min^{-1}); (b) on cooling (rate 20°C min^{-1})

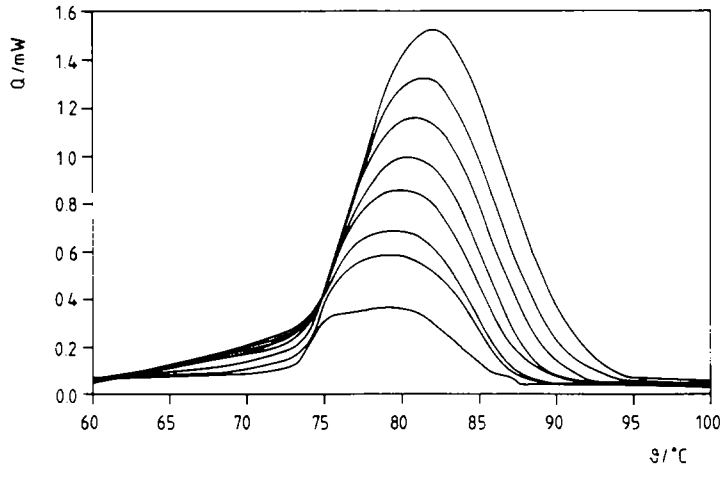

Figure 16 Differential scanning calorimetry thermograms of a 1.15 g ml^{-1} CTC–MAA solution at various heating rates (from bottom to top: 9, 16, 20, 25, 30, 36, 42 and 49°C min^{-1})

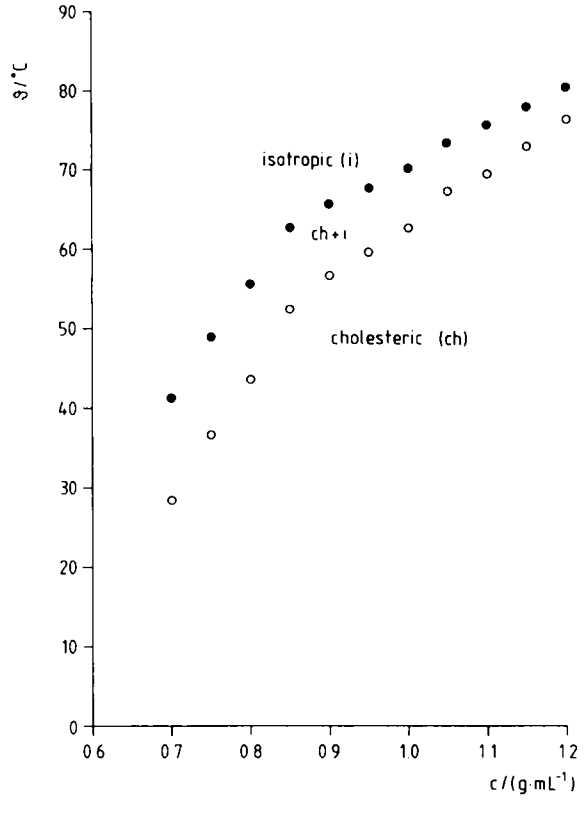

Figure 17 Phase diagram determined by d.s.c. measurements

of the phase diagram. The start of the phase transition is determined by T_{onset} provided that the slowness of the calorimeter which is due to heat transport phenomena can be excluded. The transition is theoretically finished at the d.s.c. peak maximum. The two-phase region is thus characterized by the temperature difference $\Delta T = T_{peak} - T_{onset}$. The above assumption is only valid for very slow heating, that is for a heating rate $\dot{T} \rightarrow 0$. Each sample of the series of experiments has been measured at different heating rates and T_{onset} and T_{peak} were extrapolated to $\dot{T} \rightarrow 0$. The dependence of the endothermic peaks on the heating rate is demonstrated for a solution of 1.15 g ml^{-1} in *Figure 16*. The heating rates were varied from 9 to 49°C min^{-1}. The shift of the onset and peak maximum occurs linearly with the heating rate for lyotropic CTC–MAA solutions. This behaviour seems to contradict considerations by Gray and Illers[37,38], who predicted T_{peak} or $T_{onset} \propto T^{\frac{1}{2}}$. However, this functionality is only valid for isothermal first-order transitions and does not hold for the non-isothermal liquid crystalline–isotropic transition of the CTC–MAA system. The extrapolated T_{onset} and T_{peak} to $\dot{T} \rightarrow 0$ are represented in the phase diagram (*Figure 17*) as a function of CTC concentration. The lower coexistence line, which symbolizes the beginning of the phase transition, agrees with the results from polarization microscopy (*Figure 10*) and refractometric (*Figure 13*) measurements within the limits of experimental errors. The upper coexistence line, defined by T_c, is shifted to lower temperatures compared with that obtained by the other two methods, resulting in a smaller two-phase region. This may indicate that a non-isothermal phase transition is completed at higher temperatures than the peak maxima. This problem can be solved by coupled d.s.c. and polarization microscopy measurements.

Differential scanning calorimetry investigations offer, besides the evaluation of phase diagrams, the possibility of determining the order of the liquid crystalline–isotropic phase transition for the CTC–MAA system. According to Navard and Haudin[39,40], a number N can be defined as $N = h'/h$ where h is the peak height and h' is the peak height with double the heating rate. The value of N varies between 1 and $\sqrt{2}$ for a first-order phase transition and is 2 for a second-order transition or a non-isothermal first-order transition (e.g. materials with impurities). Various pairs of heating rates have been selected for liquid crystalline CTC–MAA solutions at each concentration with a factor of 2. The number N has been calculated from the ratio of heights of corresponding peaks. On heating, that is at the anisotropic–isotropic phase transition, N does not depend on the concentration of the lyotropic solutions or on the selected heating rate pair and equals 1.9–2. On cooling, N decreases with higher concentrations and with higher heating rate pairs and has a minimum value of 1.27. At higher concentrations, the above supercooling effect increases and the two-phase region becomes smaller. The value of $N = 1.27$ for high concentrations and high cooling rates signifies that the region of coexistence vanishes completely and an isothermal first-order phase transition occurs with an enthalpy of formation. Since the measured enthalpies for the system CTC–MAA appear indepen-

dently from the direction of the transition (cooling or heating), the corresponding endothermic procedure can also be considered as a first-order transition with an enthalpy of formation but spread over a wider temperature range. The observed values for $N = 1.9$–2 on heating reflect, not as assumed in the literature, a second-order transition, but rather have to be attributed to the existence of a two-phase region.

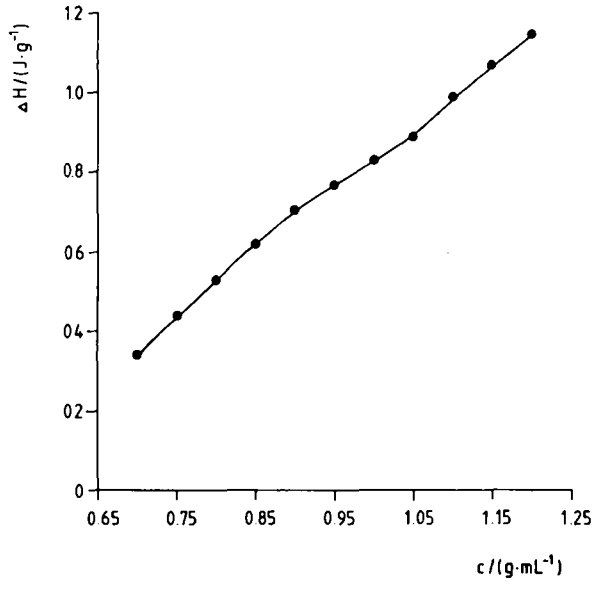

Figure 18 Phase transition enthalpies of the cholesteric–isotropic transition of CTC–MAA for various concentrations on heating or cooling

The enthalpies derived from the endothermic and exothermic d.s.c. peaks augment with increasing CTC concentrations for the samples in the series of experiments (*Figure 18*), although the degree of order for the samples is almost identical at the beginning of the transition. This may be explained by:

1. Polymer–solvent interactions diminish with higher concentration in favour of polymer–polymer contacts. Consequently larger anisotropic dispersion forces have to be overcome at the transition in the isotropic solution.
2. An increasing steric hindrance has to be overcome at the phase transition when the molecules with increasing numbers per unit volume turn into an irregular distribution.
3. The changes in the degree of order, and with it the entropy ΔS, are inversely proportional to the temperature at the transition ($\Delta S = \Delta H/T$). A higher enthalpy is needed for transitions at higher temperatures (higher concentrations) with a constant ΔS.
4. The degree of order determined by birefringence leads only to the orientation of the molecules within the nematic sheets of the cholesteric phases. The stability

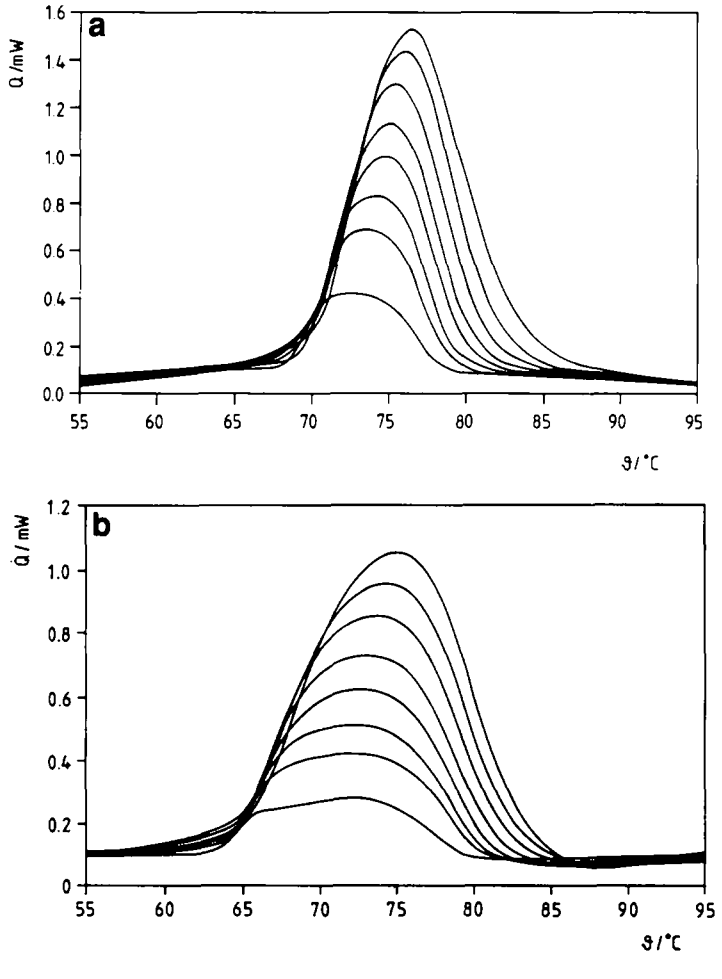

Figure 19 Differential scanning calorimetry thermograms of 1.0 g ml^{-1} CTC–MAA solutions at various heating rates (from bottom to top: 9, 16, 20, 25, 30, 36, 42 and 49°C min^{-1}): (a) CTC fraction ($M_w/M_n = 1.4$); (b) polydisperse CTC ($M_w/M_n = 6$)

perpendicular to these planes may vary with increasing concentrations.

Finally, the influence of the molar mass distribution is discussed. *Figure 19a* represents the endothermic peaks for a 1.0 g ml^{-1} CTC–MAA solution with a molar mass CTC fraction ($M_w/M_n = 1.4$). A comparison with a polydisperse CTC sample ($M_w/M_n = 6$) of the same concentration (*Figure 19b*) reveals that the beginning of the phase separation is shifted to higher temperatures, but the other parts of the curves appear almost identical. A smaller two-phase region results. Both d.s.c. investigations and temperature-dependent measurements of the degree of order prove that the molar mass distribution plays a decisive role in the size of the two-phase region.

REFERENCES

1 Bhadani, S. N., Tseng, S. and Gray, D. G. *Makromol. Chem.* 1983, **184**, 1727
2 Kamide, K., Okajima, K., Matsui, T. and Kajita, S. *Polym. J.* 1986, **18**, 273
3 Marsano, E., Bianchi, E. and Ciferri, A. *Macromolecules* 1983, **17**, 2886
4 Fried, F., Gilli, J. M. and Sixou, P. *Mol. Cryst. Liq. Cryst.* 1983, **98**, 209
5 Fried, F. and Sixou, P. *J. Polym. Sci., Polym. Chem. Edn.* 1984, **22**, 239
6 Pawlowski, W. P. and Gilbert, R. D. *J. Polym. Sci., Polym. Phys. Edn.* 1987, **25**, 2293
7 Pawlowski, W. P. and Gilbert, R. D. *J. Polym. Sci., Polym. Phys. Edn.* 1988, **26**, 1101
8 Ritcey, A. M. and Gray, D. G. *Macromolecules* 1988, **21**, 1251
9 Bhadani, S. N. and Gray, D. G. *Makromol. Chem., Rapid Commun.* 1982, **3**, 449
10 Vogt, U. *Dissertation* TU Clausthal, Clausthal-Zellerfeld, 1985
11 Steinmeier, H. *Dissertation* TU Clausthal, Clausthal-Zellerfeld, 1988
12 Siekmeyer, M. and Zugenmaier, P. *Makromol. Chem., Rapid Commun.* 1987, **8**, 511
13 Siekmeyer, M. *Dissertation* TU Clausthal, 1989
14 De Vries, Hl. *Acta Cryst.* 1951, **4**, 219
15 Haurand, P. and Zugenmaier, P. *Carbohydr. Res.* 1987, **160**, 369
16 Robinson, C. *Tetrahedron* 1961, **13**, 219
17 Onogi, Y., White, J. L. and Fellers, J. F. *J. Polym. Sci., Polym. Phys. Edn.* 1986, **18**, 663
18 Kimura, H., Hosino, M. and Nakano, H. *J. Phys. (France)* 1979, **40**, C3-174
19 Kimura, H., Hosino, M. and Nakano, H. *J. Phys. Jpn.* 1982, **51**, 1584
20 Predel, B. 'Heterogene Gleichgewichte, Grundlagen und Anwendungen' Steinkopff-Verlag, Darmstadt, 1982
21 Onsager, L. *Ann. NY Acad. Sci.* 1949, **51**, 627
22 Khokhlov, A. R. and Semenov, A. N. *Physica* 1981, **108A**, 546
23 Zugenmaier, P. *J. Appl. Polym. Sci., Appl. Polym. Symp.* 1983, **37**, 223
24 Flory, P. J. *Proc. R. Soc. London (A)* 1956, **234**, 73
25 Flory, P. J. and Ronca, G. *Mol. Cryst. Liq. Cryst.* 1979, **54**, 289
26 Flory, P. J. *J. Am. Chem. Soc.* 1976, **17**, 46
27 Flory, P. J. and Ronca, G. *Mol. Cryst. Liq. Cryst.* 1979, **54**, 311
28 Warner, M. and Flory, P. J. *J. Chem. Phys.* 1980, **73**, 6327
29 Conio, G. Bianchi, E., Ciferri, A., Tealdi, A. and Aden, M. A. *Macromolecules* 1983, **16**, 1264
30 Laivins, G. V. and Gray, D. G. *Macromolecules* 1985, **18**, 1753
31 Flory, P. J. and Frost, R. S. *Macromolecules* 1978, **11**, 1126
32 Frost, R. S. and Flory, P. J. *Macromolecules* 1978, **11**, 1134
33 Moscicki, J. K. and Williams, G. *Polymer* 1981, **22**, 1451
34 Bheda, J., Fellers, J. F. and White, J. L. *Colloid Polym. Sci.* 1980, **258**, 1335
35 Haller, I. *Prog. Solid State Chem.* 1975, **10**, 103
36 Papkov, S. P. *Adv. Polym. Sci.* 1984, **59**, 75
37 Gray, A. P. in 'Analytical Calorimetry' (Eds. R. S. Porter and J. F. Johnson), Plenum Press, New York, 1968, p. 209
38 Illers, K.-H. *Eur. Polym. J.* 1974, **10**, 911
39 Navard, P. and Haudin, J. M. *J. Therm. Anal.* 1984, **29**, 405
40 Navard, P. and Haudin, J. M. *J. Therm. Anal.* 1984, **29**, 415